Tumorigenic Potential of miR-18A* in Glioma Initiating Cells Requires NOTCH-1 Signaling

Laurent Turchi, David N. Debruyne, Fabien Almairac, Virginie Virolle, Mohamed Fareh, Yasmine Neirijnck, Fanny Burel-Vandenbos, Philippe Paquis, Marie-Pierre Junier, Ellen Van Obberghen-Schilling, Hervé Chneiweiss, Thierry Virolle

STEM CELLS®

CANCER STEM CELLS

Tumorigenic Potential of miR-18A* in Glioma Initiating Cells Requires NOTCH-1 Signaling

LAURENT TURCHI,[a,b] DAVID N. DEBRUYNE,[a,b] FABIEN ALMAIRAC,[a,b,c] VIRGINIE VIROLLE,[a,b] MOHAMED FAREH,[a,b] YASMINE NEIRIJNCK,[a,b] FANNY BUREL-VANDENBOS,[a,b,d] PHILIPPE PAQUIS,[a,b,c] MARIE-PIERRE JUNIER,[e] ELLEN VAN OBBERGHEN-SCHILLING,[a,b] HERVÉ CHNEIWEISS,[e] THIERRY VIROLLE[a,b]

[a]Université de Nice-Sophia Antipolis and [b]Institut de Biologie Valrose, CNRS UMR7277, INSERM UMR1091, Nice, France; [c]Service de Neurochirurgie and [d]Service d'Anatomopathologie, Hôpital Pasteur, CHU de Nice, Nice, France; [e]Plasticité Gliale, Centre de Psychiatrie et Neurosciences, UMR 894 INSERM/Faculté de Médecine, Université Paris Descartes, Paris, France

Key Words. miR-18a* • Delta like 3 protein • Glioblastoma • NOTCH • Sonic hedgehog • Extracellular signal-regulated kinase

ABSTRACT

Stem cell-like properties of glioma initiating cells (GiCs) fuel glioblastoma (GBM) development by providing the different cell types that comprise the tumor. It is therefore likely that the molecular circuitries that regulate their decision to self-renew or commit to a more differentiated state may offer targets for future innovative therapies. In previous micro-RNA profiling studies to search for regulators of stem cell plasticity, we identified miR-18a* as a potential candidate and its expression correlated with the stemness state. Here, using human GiCs we found that miR-18a* expression promotes clonal proliferation in vitro and tumorigenicity in vivo. Mechanistically, ERK-dependent induction of miR-18a* directly represses expression of DLL3, an autocrine inhibitor of NOTCH, thus enhancing the level of activated NOTCH-1. Activated NOTCH-1 in turn is required for sustained ERK activation. This feed-forward loop, driven by miR-18a*, is required to turn on the SHH-GLI-NANOG network, essential for GiC self-renewal. Hence, by tightly regulating expression of DLL3, miR-18a* constitutes an important signaling mediator for fine tuning the level of GiC self-renewal. STEM CELLS *2013;31:1252–1265*

Disclosure of potential conflicts of interest is found at the end of this article.

INTRODUCTION

The notion of cancer stem cell suggests that there is a hierarchical organization of cells within a tumor where only subpopulation of stem-like cells, the tumor initiating cells (TiCs), have unlimited capacity for self-renewal and are responsible for tumor initiation and maintenance [1]. According to this model, the targeting of tumor stem cells is viewed as a major therapeutic challenge. For the development of novel prospective treatments it is, therefore, necessary to understand the mechanisms involved in TiC maintenance and self-renewal [2, 3]. Cell populations that display TiC characteristics have been found in most human cancers including leukemia [4], breast cancer [5], melanomas [6], and brain tumors [7]. While it is possible to enrich for TiCs in many tumors using a number of cell surface markers such as CD133, there is compelling evidence that a fraction of the $CD133^-$ population might similarly exhibit TiC properties. Subtypes of TiCs have been isolated from glioblastoma (GBM) according to their CD133 status [8, 9] and some GBM $CD133^-$ cells are capable of long-term self-renewal and initiation of a heterogeneous tumor when xenotransplanted [8–11]. Thus, self-renewal and tumor initiation properties may not be restricted to a uniform cell population, but rather they may be displayed by a heterogeneous population. This heterogeneity is illustrated by the multiplicity of signaling systems which control self-renewal, stemness and tumorigenic properties, including NOTCH [12], extracellular signal-regulated kinase (ERK), [13], and Hedgehog pathways [14, 15]. Whether these pathways are independent and compensatory, or whether they exhibit a complex interplay is poorly described to date.

By miRNA profiling in glioma initiating cell (GiC) [16], we previously identified miR-18a* as a potential regulator of GiC plasticity. Here we examined the effect of miR-18a* on clonal prolifieration in vitro and on tumor promotion in vivo. By taking advantage of the ability of GICs to turn on and turn off their self-renewing property, we uncovered a novel molecular mechanism underlying the control of GiC stemness

Author contributions: L.T. : conception and design, manuscript writing, data analysis and interpretation, and collection and or assembly of data; D.N.D.: conception and design, data analysis and interpretation, and collection and or assembly of data; F.A., V.V., M. F., and Y.N.: conception and design and data analysis and interpretation; F.B. and M.J.: provision of study material of patients and data analysis and interpretation; P.P.: provision of study material of patients; E.V.O.: manuscript writing; H.C.: provision of study material of patients and manuscript writing; T. V.: conception and design, manuscript writing, data analysis and interpretation, collection and or assembly of data, and final approval of manuscript.

Correspondence: Thierry Virolle, Ph.D., Institut de Biologie Valrose, CNRS UMR7277, INSERM UMR1091, UNS, Parc Valrose, 06108 Nice, France. Telephone: 04 93 37 76 20; e-mail: virolle@unice.fr. Received September 24, 2012; accepted for publication February 28, 2013; first published online in STEM CELLS *EXPRESS* March 26, 2013. 1066-5099/2013/$30.00/0 doi: 10.1002/stem.1373

and tumorigenicity. We demonstrate a positive regulatory feedback between ERK and NOTCH pathways which strongly relies on miR-18a*-mediated repression of delta like 3 protein (DLL3) expression. Importantly this mechanism is necessary to turn on the sonic hedgehog (SHH)-GLI-NANOG signaling network, which is essential for the maintenance of GiCs [14, 15]. Our findings provide mechanistic insights into tumor cell plasticity and highlight a key miRNA-dependent control of stemness and the self renewal status of GiC.

Materials and Methods

Cell Culture

Patient-derived cells were isolated from surgical resections of human primary GBM provided by the Neurosurgery Departments of St Anne Hospital in Paris (TG1 and TG6 cells [17]) and the CHU of Nice (GB1 and GB3 cells, from 62- and 71-year-old male patients, respectively). According to the Verhaak classification [18], all cells display a gain on chromosome 7, a loss on chromosome 9p, no mutation of *IDH1*, active SHH and NOTCH pathways. *TP53* is not mutated, except in GB3 cells, which bear a G244S p53 mutation. GB1 and GB3 cells also display a loss on chromosome 10. TG1 and TG6 cells were shown to initiate tumors when orthotopically grafted (<500 cells) in immune-compromised mice [17]. As self-renewing GiCs, TG1, TG6, GB1, and GB3 cells grow as neurospheres in serum-free defined medium as described elsewhere [17]. For differentiation experiments, neurospheres were dissociated and 5×10^5 cells were seeded in fetal calf serum medium (MFCS) (Dulbecco's modified Eagle's medium [DMEM]-F12, 10 mM glutamine, 10 mM HEPES, 0.025% sodium bicarbonate, 0.5% fetal calf serum (FCS)). Where indicated, cells were treated with U0124 or U0126 (15 μM) or LY-374973, N-[N-(3,5-Difluorophenacetyl)-L-alanyl]-S-phenylglycine t-butyl ester (DAPT) (10 mM). For GB1 and GB3, the results showing their ability to self-renew, to lose stemness markers upon serum treatment, as well as their capability to survive and infiltrate in mouse brain tissues are shown in Supporting Information Figure S1.

Plasmid Constructs and Stable Cell Lines

Full length DLL3cDNA was obtained from Origene (Rockville, MD, http://www.origene.com/orf). The DLL3 coding sequence (DLL3CS) and 3′-UTR (wt) were subcloned in pCMV and psi-Check, respectively. The constructs pDLL3mut and DLL3 3′-UTR deleted for the miR18a* seed (Del) were, respectively, obtained by site directed mutagenesis using the following oligos: olDLL3mut: 5′-ctcaagggatctacgttatctccgctccttc-3′; olDEL: 5′-tactcagcggggaggcagcctctctaatg-3′.

Synthetic double-strand DNA sequences for miR-18a/a* precursor and control nonrelevant single hairpin RNA (shRNA) (sh-CTL) (Eurogentec S.A.) were cloned in pEnter H1/T02 (ref K4920-00, Life Technologies, Rockville, MD, http://www.life-tech.com) and then subcloned in the 2K7 blasticidin lentiviral vector (2K7BSD) by recombination in presence of LR clonase II (ref 11791-020, Life Technologies). Lentiviral particles were produced by transfection of 2K7BSD-miR-18a* or 2K7BSD-sh-Ctl constructs along with the packaging vectors in the 293T cell line. After lentiviral infection, stable cell lines expressing miR-18a* (TG6 miR-18a*/TG1 miR-18a*) or the control sh-CTL (TG6 CTL/TG1 CTL) were selected in neurobasal medium (NBE) containing 1 μg/mL blasticidin for at least 15 days. Two stable cell lines generated separately from different viral productions/infections displayed the same behavior. Stable expression of sh-ERK1 and sh-ERK2 in TG1 and TG6 has been carried out as described [20].

Western Blot Analysis

Total proteins were extracted from GiCs at the indicated times, culture conditions, and treatment (buffer : 50 mM Tris-Hcl pH 7.6, 150 mM NaCl, 5 mM EDTA, 1% Nonidet P40). After migration on SDS-polyacrylamide gels, proteins were transferred to Immobilon P membranes (Millipore, Bedford, MA, http://www.millipore.com) and probed with rabbit polyclonal antibodies to active-phospho-ERK (ref V8031, Promega, Madison, WI, http://www.promega.com) or ERK1 (ref sc93, Santa Cruz Biotechnology, Santa Cruz, CA, http://www.scbt.com), mouse antibody to ERK2 (ref sc1647, Santa Cruz), or rabbit monoclonal antibody to C-term DLL3 (ABGENT, Interchim, http://www.abgent.com).

Immunofluorescence

Cells were seeded on polylysine-coated glass coverslips in NBE or MFCS. At the indicated time, cells were fixed with methanol (5minutes at −20°C). Blocking and staining were performed in phosphate buffer saline (PBS) containing 10% FCS and 0.1% Triton X-100 with the following primary antibodies: goat antibodies to SHH (C18) (1/20 dilution, sc1195, Santa Cruz); goat antibodies to Nanog (5 μg/mL, AF1997, R&D Systems,, Minneapolis, MN, http://www.rndsystems.com); rabbit antibodies to active NOTCH-1 (1/100 dilution; Abcam, Paris, France, http://www.abcam.com). SHH and DLL3 (DLL3 C-term antibody clone RB23871, ref AP9328b, ABGENT) double-immunolabelings were performed on paraffin-embedded GBM sections (selected from the database of the Department of Pathology, CHU-Nice). Nuclei were stained with 4′,6′-diamidino-2-phenylindole (DAPI). Fluorescence was observed on a Nikon Eclipse Ti inverted microscope.

Clonogenic Assay

Neurospheres were dissociated by pipeting gently up and down to obtain single cells. Cells were serially diluted and seeded in 96-well plates (one cell per well) in defined medium, or in serum containing medium (DMEM, 0.5% serum). When indicated, the cells were cultured in serum-containing medium for 4 days prior to being switched to defined medium NBE. In some experiments, cells were seeded under similar conditions in the presence or absence of MEK (U0126) or NOTCH (DAPT) inhibitors. After 3 weeks, each plate was observed and the number of neurospheres was assessed and quantified.

Quantitative Real-Time Reverse Transcription Polymerase Chain Reaction

RNAs were extracted using Trizol reagent. MicroRNA and mRNA expression levels were quantified by real-time two step reverse transcription polymerase chain reaction (RT-PCR). Reverse transcription steps were performed with Superscript II reverse transcriptase and Taqman Reverse transcription microRNA kit (ref 4366596, Life Technologies, http://www.lifetechnologies.com/fr/fr/home.html?s_kwcid=TC%7c12170%7clife%2520-technologies%7c%7cS%7ce%7c17677724708) for mRNA and miRNA, respectively, accordingly to the manufacturer's instructions. Real-time PCR was performed with universal Taqman PCR Master Mix (Life Technologies). The expression of each gene was determined relative to U54 expression as an internal control. Fold stimulation was calculated using the ΔΔCT method.

small interfering RNA (siRNA) and Anti-miR Cell Transfection

GiCs in NBE or serum-containing medium were transfected with lipofectamine 2000 (Life Technologies) according to manufacturer's instructions 24 hours before the end of the experiment or the epidermal growth factor (EGF) stimulation. Stealth siRNA (Life Technologies) is located at position 1,725 in DLL3 mRNA (the sequence is not available). Anti-miR-18a* and scrambled sequences were from Ambion (Austin, TX, http://www.ambion.com).

Orthotopic Xenografts

2×10^5 TG1 control or TG1 miR-18a* cells and 50,000 or 500 TG6 control or TG6 miR-18a* were resuspended in 5 μL of Hanks balanced salt solution (Life Technologies) and stereotactically implanted unilaterally into the striatum of male NOD.CB17-Prkdcscid/NCrHsd mice (Harlan Laboratories). According to a protocol approved by the local institutional animal care and experimentation committee, Trypan blue staining was performed prior injection to assess cell viability. TG1 cells stably expressed a luciferase reporter gene, which allowed tumor detection in living animals. Two groups of five mice were injected. Cell survival and tumor growth were monitored and quantified in the living animals using the IVIS Lumina II system (Caliper Life Sciences).

miRNA In Situ Hybridization

The experiments were carried out with the miRCURY LNA microRNA ISH Optimization Kit (FFPE) as indicated by Exiqon (Exiqon A/S Skelstedet). Briefly, sections of paraffin-embedded glioma samples (selected from the database of the Department of Pathology, CHU-Nice) were deparaffinized in xylene, hydrated in successive ethanol baths (99%–70%), and rinsed in PBS. Rehydrated sections were treated with proteinase K at a final concentration of 15 μg/mL for 10 minutes at 37°C and washed with PBS. Slides were dehydrated in ethanol (70%–99%) and air dried. Slides were hybridized with hsa-miR-18a*miRCURY LNA detection probe (ref 38781-15 Exiqon) at a final concentration of 10 nM at 55°C in a humidified chamber then washed by successive incubations with 5× saline-sodium citrate (SSC) to 0.2× SSC. Slides were then incubated with anti-DIG antibody diluted at 1/800 in the blocking solution for 1 hour at room temperature then washed with 0.1% Tween PBS. Slides were then incubated with nitro blue tetrazolium (NBT) and 5-bromo-4-chloro-3-indolyl phosphate (BCIP) alkaline phosphate substrate containing 0.2 mM levamisol, for 1 hour at 37°C to reveal anti-DIG antibody and double DIG miRCURY LNA probe immuno-complexes. Nuclei were stained with Nuclear fast red and then slides were dehydrated and mounted with mounting medium (Eukitt, Sigma-Aldrich, St. Louis, http://www.sigmaaldrich.com).

RESULTS

MiR-18a* Promotes GiC Clonal Proliferation and Tumorigenicity

We have previously described that GiCs cultured in serum-containing medium became committed to a more differentiated state, lost the SHH-NANOG regulatory network [16], and consequently were incapable of self-renewal (Fig. 1A–1C) [14, 15]. Under these conditions we observed the repression of miR-18a* expression, as compared to cells cultured in serum-free defined medium appropriate for self-renewal of adult neural stem cells (Fig. 1D). Using four different patient-derived primary GiC cultures isolated from primary GBM (TG1, TG6 [17], GB1, GB3), we further showed that the serum-induced loss of clonal proliferation may be totally rescued if the cells are switched to defined medium (Fig. 1C). Upon this treatment, expression of SHH and NANOG were efficiently restored at the mRNA and protein levels (Fig. 1A, 1B). Although only 0.35% and 0.47% of the serum-differentiated TG1 population was positive for SHH and NANOG, 97% and 98% of the cells expressed these markers after 48 hours of dedifferentiation (Supporting Information Fig. S2A). The same results were obtained using TG6, GB1, and GB3 (Supporting Information Fig. S2A). A similar enrichment was also observed using OCT4 as a stemness marker (Supporting Information Fig. S2B). Interestingly, video microscopy of the switch from serum-containing to defined medium (from 0 to 8 hours) showed that dedifferentiated cells had the same capacity as original GiCs to form neurospheres (Supporting Information Fig. S2B). To demonstrate that enrichment of stemness markers resulted from cell dedifferentiation, and not clonal expansion of remaining self-renewing cells, we labeled differentiated cells with carboxyfluorescein diacetate, succinimidyl ester (CFSE) and compared levels of fluorescence after the switch to defined medium for 48 hours. An equivalent staining and cell distribution (Fig. 1E, table 1) demonstrated that enrichment of stemness markers was independent of proliferation and was rather due to a conversion to the stemness state.

Interestingly, miR-18a* was also stimulated after the replacement of serum medium with defined medium (Fig. 1D; Supporting Information Fig. S2C). miR-18a* expression may therefore be correlated with the self-renewal ability of cells and may somehow contribute to clonal proliferation and tumorigenic potential of GiCs. To test this hypothesis, we generated modified TG1 and TG6 cells (TG1 miR-18a*; TG6 miR-18a*), which stably and constitutively overexpress miR-18a*, approximately sixfold above the levels observed in control cells (TG1 ctl; TG6 ctl) infected with a nonrelevant construct (Supporting Information Fig. S2D, S2E). We first assessed the clonal proliferation of each cell line and observed that miR-18a* overexpression significantly increased cloning efficiency by 16% (70% for TG1 ctl vs. 86% for TG1 miR-18a*, p value = .0002) and 15% (69.4% for TG6 ctl vs. 84.6% for TG6 miR-18a*, p value = .00007) for TG1 and TG6 cells, respectively (Fig. 1F). In addition, bromodéoxyuridine (Brdu) staining revealed that cells overexpressing miR-18a* displayed a proliferation rate that was 10% higher than in control cells (Fig. 1G). Constitutive miR-18a* overexpression leads, therefore, to increased cell proliferation and clonogenicity. We then grafted either TG1 ctl or TG1 miR-18a* cells in the cortex of immunocompromised mice Nonobese diabetic-severe combined immunodeficient (NOD/SCID) to test their tumorigenicity. Tumor development was monitored in live animals by measuring the activity of a luciferase reporter gene constitutively expressed in each cell line. As shown in Figure 1H, overexpression of miR-18a* significantly increased tumor growth, compared to TG1 ctl cells. Similar results were obtained following orthotopic injection of TG6 ctl or TG6 miR-18a* cells (<500 cells), as shown in Supporting Information Fig. 2F), confirming that miR-18a* is capable of promoting GiC tumorigenicity in vivo.

MiR-18a* Expression Is Under the Control of the ERK Pathway

We next sought to determine the pathway responsible for the regulation miR-18a*. Since the mitogen-activated protein kinases (MAPK) ERK has been reported to be involved in regulation of the Hedgehog pathway [21], we examined its contribution to SHH-Gli-NANOG expression and ensuing regulation of clonal proliferation of GiCs. Therefore, we cultured TG1, TG6, GB1, and GB3 cells under serum conditions for 4 days then induced miR-18a* expression by switching them to defined medium for 48 hours, in the presence or absence of the MEK inhibitor U0126 or Parke-Davis PD98059. Inhibition of ERK phosphorylation was monitored by immunofluorescence and Western blotting (Supporting Information Fig. S3A, S3C). Quantitative PCR (qPCR) analyses revealed that ERK inhibition efficiently blocked expression of mRNA encoding SHH, as well as that of its effector GLI-1 in all of the GiCs (Fig. 2A, 2B). Accordingly, the expression of SHH and NANOG proteins was also blunted under these conditions (Fig. 2C; Supporting Information Fig. S3D). Consequently,

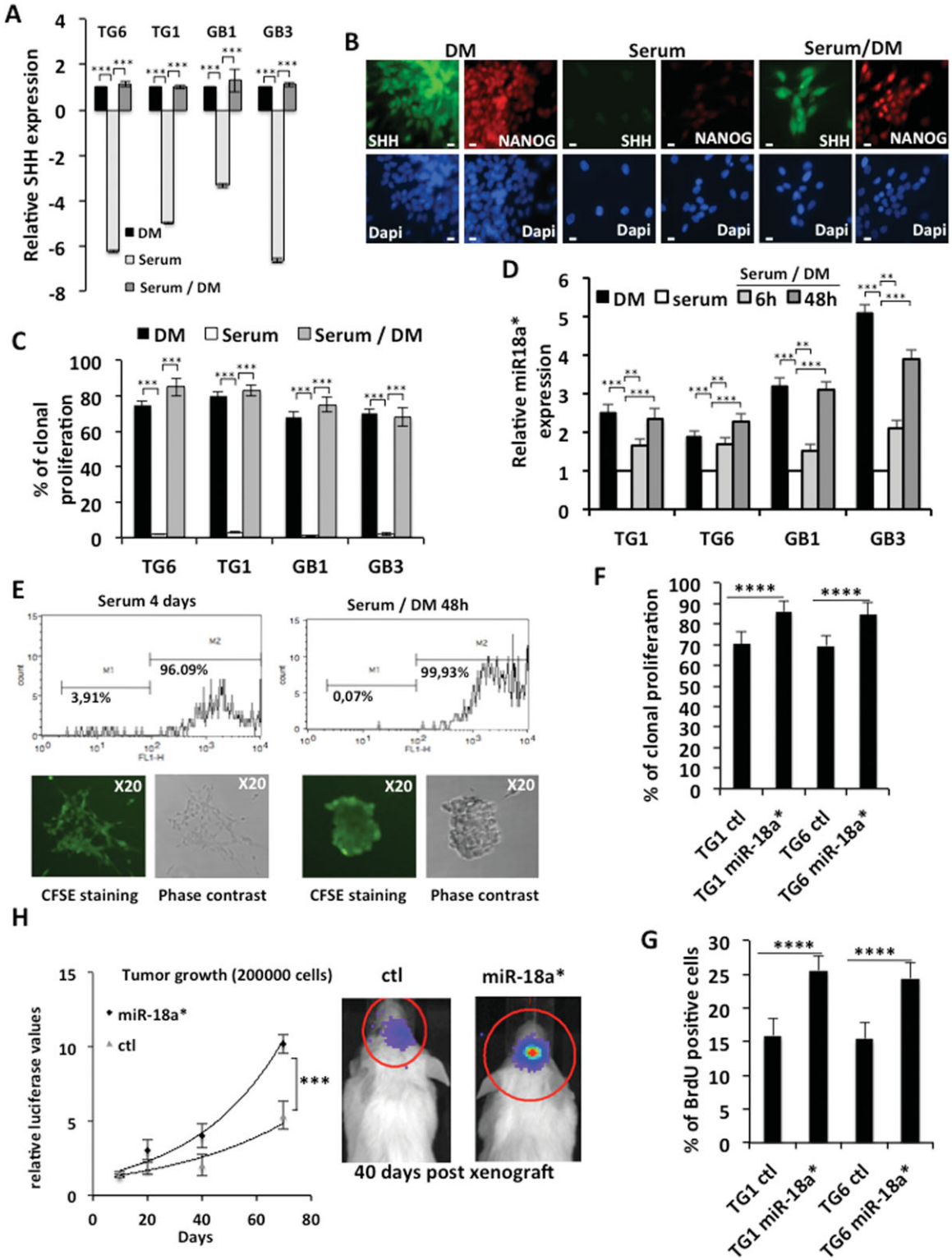

Figure 1. miR-18a* promotes clonal proliferation of glioma initiating cell (GiCs) and tumorigenicity. **(A):** Quantitative polymerase chain reaction (qPCR) analysis of sonic hedgehog (SHH) mRNA expression in four different GiC primary lines (TG6, TG1, GB1, GB3) either cultured in DM, in serum for 4 days (serum), or in serum for 4 days then in DM for 2 days (serum/DM). Results are the average of three independent experiments. **(B):** Similar culture conditions were used to assess SHH and NANOG expression by immunofluorescence in TG6 cells. Scale bar = 20 μm. The nuclei were stained with DAPI. **(C):** TG6, TG1, GB1, and GB3 cells were cultured as single cells either in DM, in serum for 4 days (serum), or in serum for 4 days then in DM (serum/DM). Hundred wells were counted for each condition to assess the clonal proliferation efficiency. Results are the average of four independent experiments. **(D):** Histogram shows HSA-miR-18a* expression in TG1, TG6, GB1, and GB3 cells either cultured in DM, in serum (serum) or cultured in serum (4 days) prior to DM for 6 or 48 hours. HSA-miR-18a* expression has been determined by qPCR using a Taqman probe as described in the Methods section. **(E):** Upper panel, fluorescence activated cell sorting (FACS) analysis displaying CFSE quantifications in cells cultured in serum for 4 days and then switched to DM for 48 hours. Lower panel, fluorescent and phase contrast images of CFSE-labeled cells. **(F):** TG1-ctl or TG1-miR-18a* and TG6-ctl or TG6-miR-18a* were seeded as single cells in DM to assess their clonal proliferation efficiency. Hundred wells were counted for each condition and the results represent the average of four independent experiments. **(G):** BrdU staining of TG1-ctl or TG1-miR-18a* and TG6-ctl or TG6-miR-18a* cells was quantified by counting fluorescent nuclei under the microscope. **(H):** TG1 cells stably expressing miR-18a* (miR-18a*), or a nonrelevant construct (ctl), were grafted in the brain of NOD/SCID mice. Both cell lines stably expressed a luciferase reporter gene. Tumor growth was assessed in living animals by measuring luciferase activity. Results represent the average of five mice for each group. (****, p value <.0001; ***, p value <.001; **, p value <.01). Abbreviations: CFSE, carboxyfluorescein diacetate, succinimidyl ester; DM, defined medium; DAPI, 4′,6′-diamidino-2-phenylindole; SHH, sonic hedgehog.

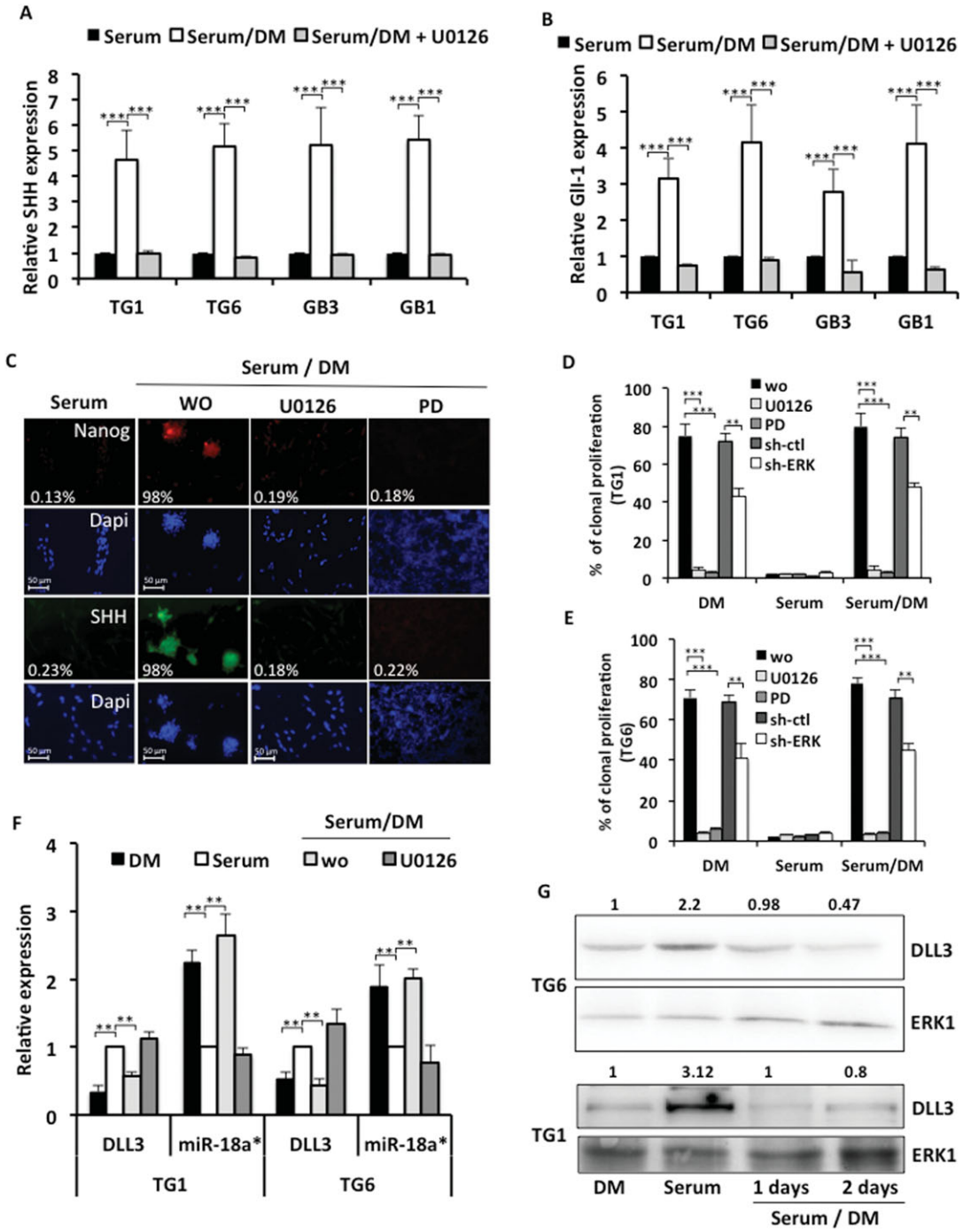

Figure 2. ERK activation is required for sonic hedgehog (SHH), GLI-1, and NANOG expression in glioma initiating cell (GiC). **(A):** SHH and **(B)** GLI-1 mRNA level were assessed by quantitative polymerase chain reaction (qPCR) in four different primary GiC lines cultured either 4 days in serum (serum) or 4 days in serum then switched to DM (serum/DM) for 48 hours. When indicated, the MEK inhibitor U0126 was added to the culture medium. **(C):** Similar conditions, plus inhibition of ERK activation with Parke Davis 98059 (PD), were used in TG6 cells to assess NANOG and SHH protein expression by immunofluorescence. The nuclei were stained with DAPI. **(D):** TG1 or **(E)** TG6 cells were cultured as single cells in DM, in the presence or absence of the MEK inhibitor U0126, Parke Davis 98059 (PD) or following shRNA-mediated silencing of ERK1/2, to assess their clonal proliferation efficiency. Hundred wells were counted for each condition. Results are the average of four independent experiments. **(F):** TG1 and TG6 cells were cultured either in DM, for 4 days in serum (serum) or for 4 days in serum then in DM (serum/DM) for 48 hours. The U0126 was added in the medium where indicated. qPCR analysis using Taqman probes show the miR-18a* and DLL3 expression in these conditions. **(G):** TG6 and TG1 cells were cultured in DM, in serum for 4 days (serum), or cultured in serum for 4 days then in DM (serum/DM) for 1 and 2 days. DLL3 expression in protein extracts was assessed by Western blotting. Western blot quantifications (image J software) are indicated above the lanes. (***, p value $<.001$; **, p value $<.01$). Abbreviations: DM, defined medium; DAPI, 4′,6′-diamidino-2-phenylindole; ERK, extracellular signal-regulated kinase.

clonal proliferation was drastically repressed following inhibition of ERK signaling (Fig. 2D, 2E; Supporting Information Fig. S3I, S3J). Interestingly, miR-18a* repression upon serum treatment could not be reversed by defined medium when ERK was inactivated (Fig. 2F). Similar results were obtained when RNAi-based silencing was used instead of U0126 to inhibit ERK phosphorylation (Fig. 2D, 2E; Supporting Information Fig. S3F–S3H). Thus, the ERK pathway plays a major role in controlling the clonal proliferation of GiCs through tight regulation of the SHH-GLI-NANOG regulatory network. In that context, our results suggest miR-18a* is an effector of ERK. To identify miR-18a* targets, we performed microarray profiling of mRNAs that were downregulated by switching from serum-containing to defined medium (48 hours) but remained unchanged when ERK was inhibited (data not shown). Examination of the microarray data in silico (target scan) revealed 10 putative miR-18a* targets. Since the NOTCH pathway is required for GiC clonal proliferation and tumorigenicity [12], we focused our attention on the known inhibitor of NOTCH activity [22, 23], DLL3. qPCR and Western blot analyses confirmed the microarray data and revealed a drop in DLL3 mRNA and protein expression when cells were cultured in defined medium (Fig. 2F, 2G). This drop in DLL3 levels was totally abrogated by MEK inhibition (Fig. 2F). Thus, DLL3 and miR-18a* expression are both under the control of ERK. In addition, the inverse correlation between their expression levels strongly suggests that miR-18a* is able to regulate DLL3 expression.

MiR-18a* Directly Downregulates DLL3 Protein Levels

In order to assess the impact of miR-18a* on DLL3 expression, we performed loss of function analyses by transfecting TG1, GB1, GB3, or TG6 cells with an anti-miR-18a* probe or a scrambled probe as control (Supporting Information Fig. S4A, S4B). Thereafter, we promoted the drop in DLL3 levels by shifting cells from serum-containing to defined medium and determined the effect of miR-18a* on this response. As shown in Figure 3A, the drop in DLL3 levels was totally abolished when miR-18a* was functionally invalidated while the presence of the scrambled probe did not affect DLL3 repression. Similar results have been obtained in GB1 and GB3 (Fig. 3A). Conversely, miR-18a* overexpression abrogated DLL3 expression at both mRNA and protein levels in TG1 and TG6 cells (Fig. 3B, 3C; Supporting Information Fig. S4C). These results demonstrate the ability of miR-18a* to negatively regulate DLL3 protein expression, thus confirming miR-18a* activity. In order to assess whether this miR-18a* regulation occurs directly, we cloned the 3′ UTR of the DLL3 mRNA into a luciferase reporter construct. A similar construct lacking the sequence bound by the miR was also generated as negative control. Both constructs were transfected along with a miR-18a* synthetic sequence. Strong inhibition of luciferase activity was observed only in cells expressing the wt construct (Fig. 3D). Taken together these results clearly demonstrate the ability of miR-18a* to directly modulate DLL3 protein expression levels.

mir-18a* Constitutes an Important MAPK Effector for the Regulation of SHH Signaling

To assess the relevance of miR-18a*-mediated downregulation of DLL3 on clonal proliferation of GiCs, we first assessed the level of SHH and GLI-1 mRNA in TG1 miR-18a* and TG1 ctl cells cultured 4 days in serum conditions prior to the addition of defined medium for 48 hours. SHH and GLI-1 mRNA expression , respectively, 3.5 and 2-fold higher in TG1 miR-18a* than in TG1 ctl cells (Fig. 4A, 4B). Similar results were observed in TG6 miR-18a*. Taking advantage of the fact that TG1 miR-18a* stably expressed exogenous miR-18a* independently of MAPK activity (Supporting Information Fig. S5A), we tested whether this forced expression could be sufficient, to rescue the SHH signaling when ERK activation was inhibited. Thus, cells were treated, with U0126 or U0124, an inactive form of the inhibitor. In the absence of ERK activation, miR-18a* overexpression failed to induce SHH and GLI-1 expression (Fig. 4A, 4B) thus demonstrating the requirement of an active MAPK to turn on the SHH pathway. Similar results have been obtained using TG6. In order to confirm the impact of miR-18a* on regulation of the SHH pathway, we performed its functional invalidation using a specific anti-miR-18a* probe in similar culture conditions. Alternatively, a nonrelevant scrambled probe was used as control (Fig. 4C, 4D). While the scrambled probe had no effect, repression of miR-18a* with the antisense probe substantially decreased the levels of SHH and GLI-1 (Fig. 4C, 4D). In accordance with the miR-18a*-mediated repression of DLL3, SHH and GLI-1 expression was clearly enhanced when DLL3 was inhibited, while their levels remained unchanged by the rescue of DLL3 expression (Fig. 4C, 4D). Consequently, while NANOG protein levels were strongly repressed in absence of miR-18a* (Fig. 4E; Supporting Information Fig. S4D) its expression appeared earlier and was more robust in TG1 or TG6 miR-18a* as compared to TG1 or TG6 ctl cells (Fig. 4F; Supporting Information Fig. S4E). As shown in Figure 4A, 4B, we found that the regulation of SHH and GLI-1 expression by the miR-18a* required an activated ERK. It is, therefore, likely that miR-18a* and DLL3 levels may interfere with ERK activation. To test this hypothesis, we first compared TG1 or TG6 miR-18a* and TG1 or TG6 ctl for ERK MAPK activity 48 hours after placing cells in defined medium. Our results showed that ERK proteins were phosphorylated to a greater extent, and earlier, in TG1 and TG6 miR-18a* cells than in TG1 and TG6 ctl cells (Fig. 4G; Supporting Information Fig. S4F). Similarly, the reduction of DLL3 protein expression in naïve TG1 or TG6 cells, using specific siRNA, led to increased ERK phosphorylation (Fig. 4H; Supporting Information Fig. S4G). This gain in ERK phosphorylation was abolished by expression of a functional DLL3 construct (pDLL3mut) that is insensitive to the siRNA (Fig. 4H; Supporting Information Fig. 4G). These results suggest the existence of a miR-18a* dependent positive feedback loop affecting ERK activation.

mir-18a*/DLL3-Mediated NOTCH Activation is Required for ERK Activation, SHH-Gli-NANOG Network Expression, and Clonal Proliferation of GiCS

DLL3 is an inhibitor of NOTCH signaling when expressed in the same cell as the NOTCH receptor [22, 23]. In light of the fact that miR-18a* represses DLL3 expression, it is likely that positive regulation of NOTCH signaling by miR-18a* may contribute to the activation of the SHH-GLI-NANOG network, and thereby enhance clonal proliferation of GiCs. Immunofluorescence using an antibody specific to the activated form of NOTCH-1 revealed substantial staining of activated NOTCH-1 in self-renewing cells (Fig. 5A; Supporting Information Fig. S5B). NOTCH-1 activation, lost upon serum treatment, was totally rescued 24 or 48 hours after the change from serum to defined medium (Fig. 5A; Supporting Information Fig. S5B). Furthermore, the use of a gamma secretase complex inhibitor, DAPT, which prevents NOTCH activation and translocation into the nucleus, induced a drastic loss of

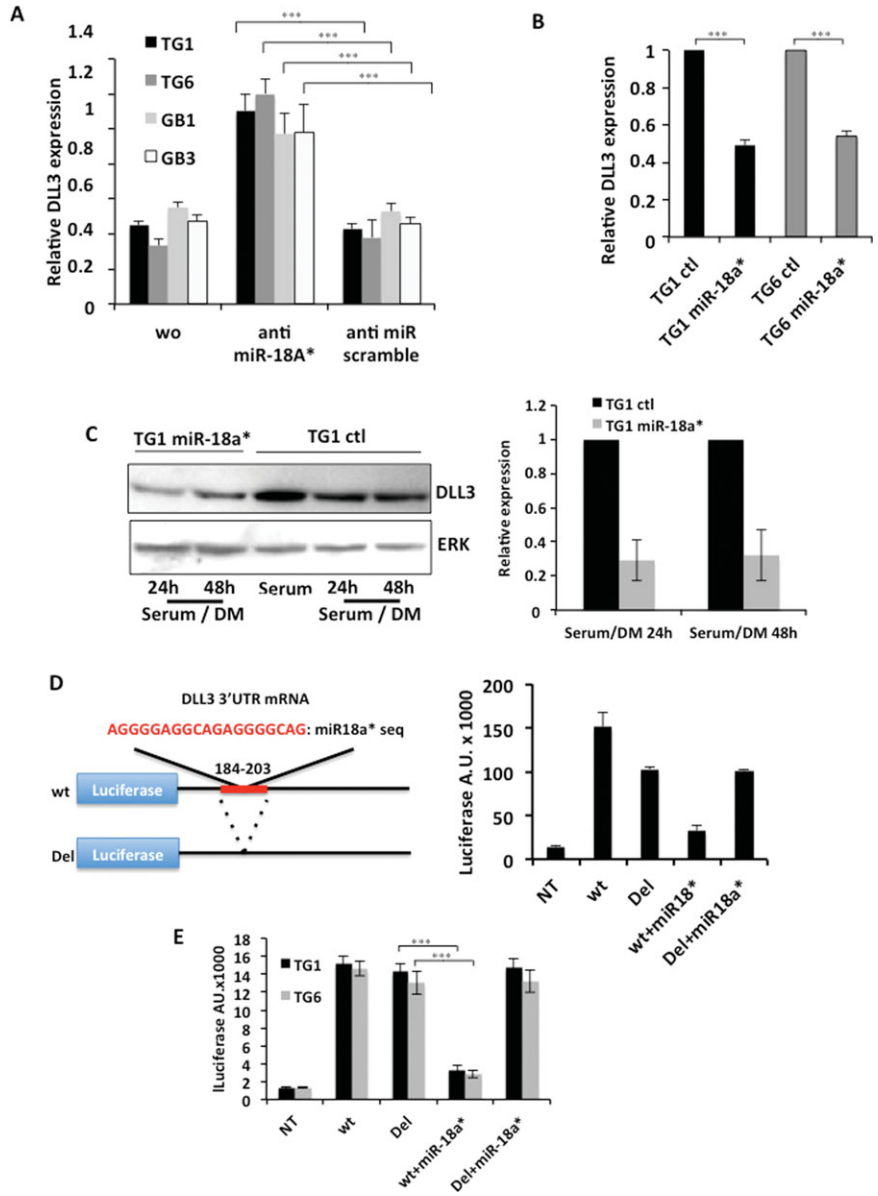

Figure 3. miR18a* directly regulates delta like protein 3 (DLL3) protein levels. **(A):** TG1, TG6, GB1, and GB3 cells were cultured in serum for 4 days, then transfected with anti miR-18a*, anti-miR scrambled or mock (WO) and then switched to DM for 2 days. DLL3 mRNA expression was assessed by quantitative polymerase chain reaction (qPCR) using a TAQMAN probe and compared to DLL3 levels measured in serum-treated cells. Results are the average of three independent experiments. **(B):** DLL3 mRNA levels were assessed by qPCR in TG1-ctl and in TG1-miR-18a* cells and in TG6-ctl and in TG6-miR-18a* cells, cultured in DM. **(C):** TG1-ctl or TG1-miR-18a* cells were cultured for 4 days in serum (serum) or 4 days in serum then switched to DM (serum/DM) for 24 or 48 hours. DLL3 protein expression was assessed in each condition by Western blotting. Antibody specific to ERK2 was used as loading control. Histogram displays the immunoblot quantification determined using Image J software (lower panel). Values are the mean of the ratio of DLL3 to total ERK2 intensities. **(D):** The DLL3 3′-UTR, wild-type (wt) or lacking the miR-18a* binding site (Del), were fused to a luciferase gene (upper panel). The resulting constructs were transfected in HEK293 cells alone or with synthetic miR-18a*. Luciferase activities were assessed 48 hours later by luminometry. Results are the average of three independent experiments. (***, p value $<.001$). Abbreviation: DM, defined medium.

mRNA encoding its known targets HES1, 2, and 5 as well as HES3 to lesser extent (Fig. 5B; Supporting Information Fig. S5C), thus demonstrating efficient activation of NOTCH signaling by the defined medium. In order to maintain a high level of DLL3 expression, we transfected a miR-18a*-insensitive DLL3 construct lacking the 3′ UTR of the gene (pDLL3-CDS) in serum-cultured TG6 or TG1 cells 24 hours prior to placing them in defined medium. Effects on NOTCH activation were assessed 24 hours later by immunofluorescence. Whereas the cells transfected with a nonrelevant plasmid displayed high levels of activated NOTCH, DLL3 overexpression strongly antagonized NOTCH activation (Fig. 5C; Supporting Information Fig. S6A). Interestingly the blockade of ERK1/2 phosphorylation led to similar effects confirming that, NOTCH activation, similar to DLL3 expression, was dependent on ERK in this system (Fig. 5C; Supporting Information Fig. S6A). Conversely, the loss of DLL3 protein in the same culture conditions led to an increase of HES1, 2, and 5 levels, confirming that activation of NOTCH signaling was strongly dependent on DLL3 levels (Fig. 5D; Supporting

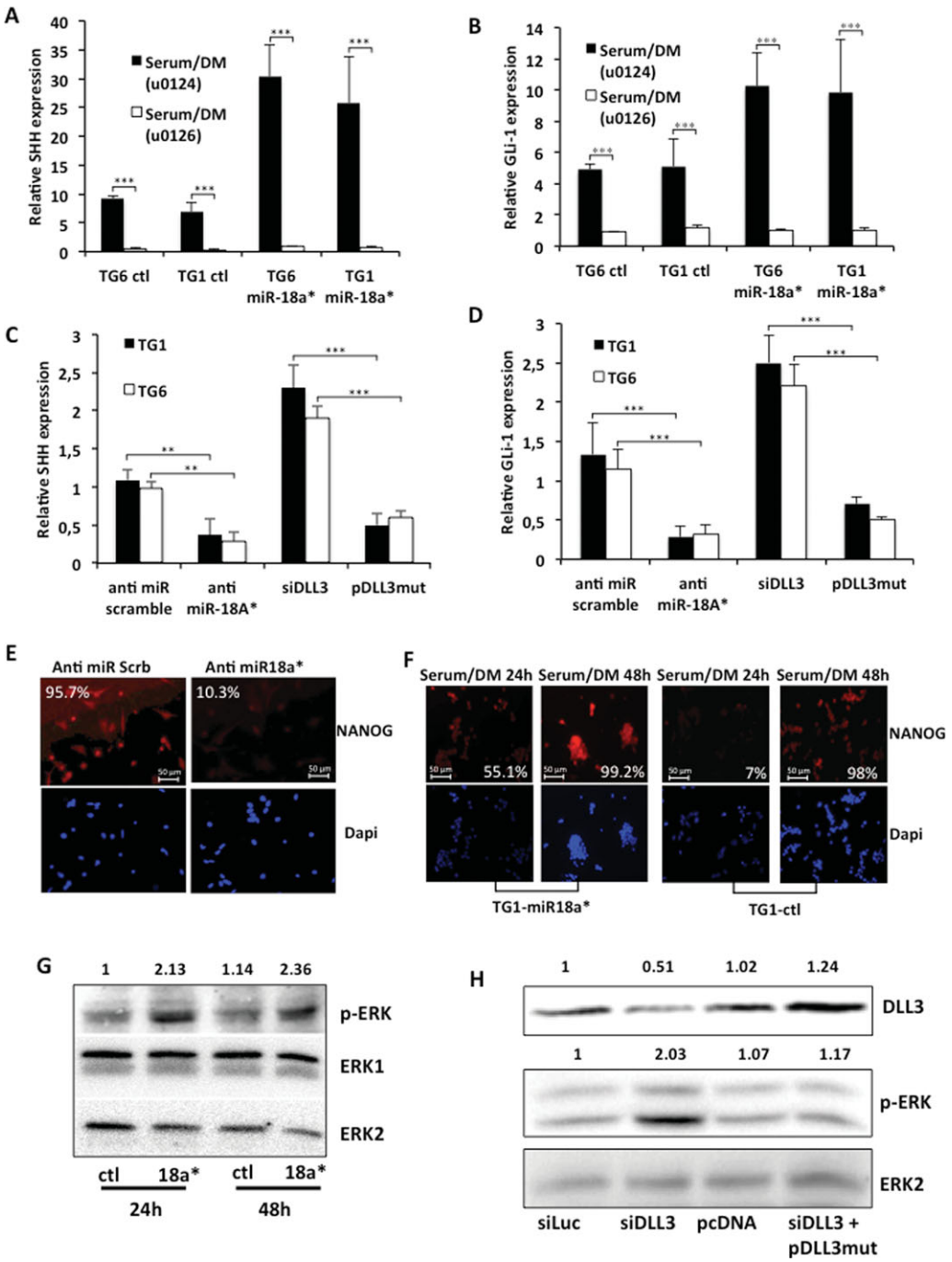

Figure 4. Modulation of miR-18a* and DLL3 expression impacts SHH-GLI-NANOG expression and ERK activation. **(A):** Sonic hedgehog (SHH) and **(B)** GLI-1 mRNA levels were assessed by quantitative polymerase chain reaction (qPCR) using TAQMAN probes in TG1-ctl, TG1-miR-18a*, TG6-ctl, or TG6-miR-18a* cells incubated 4 days in serum (serum), then cultured in DM (serum/DM) for 48 hours in the presence of U0126 or its inactive analog U0124. Values are compared to those measured in serum-treated cells. Similar culture conditions were used to assess **(C)** SHH and **(D)** GLI-1 mRNA expression by qPCR, in TG1 and in TG6 cells transfected with either anti-miR scrambled or siLuc as control and with either anti miR-18a* or siDLL3 with or without a DLL3 construct insensitive to siDLL3 (pDLL3mut). Cells were cultured 4 days in serum prior transfection and then incubated in DM for 48 hours. Each experiment has been repeated at least three times. **(E):** TG1 cells transfected with either anti-miR scrambled (Scrb) or anti-miR18a* were incubated 4 days in serum prior to being placed for 48 hours in DM. NANOG protein expression is revealed by immunostaining. Quantification of NANOG positive cells is displayed. The nuclei were stained with DAPI. **(F):** TG1-ctl or TG1-miR-18a* were incubated 4 days in serum prior to being cultured for 24 or 48 hours in DM. NANOG protein expression is revealed by immunostaining. Quantification of NANOG positive cells is displayed. **(G):** Immunoblot analyses showing the phospho-ERK levels in TG1-ctl or TG1-miR-18a* cells previously cultured in serum medium for 4 days then incubated in DM for 24 or 48 hours. Middle and lower panels display total ERK1 and ERK2 proteins. Western blot quantification, using image J software, is indicated above the lanes. **(H):** Immunoblot analyses showing DLL3 protein expression and phospho-ERK levels in TG1 cells following functional invalidation of DLL3 (siDLL3) or rescue of DLL3 expression (siDLL3 + pDLL3 mut). siLuc and pcDNA were used as control. Western blot quantifications (image J software) are indicated above the lanes. (***, p value <.001; **, p value <.01). Abbreviations: DM, defined medium; DAPI, 4′,6′-diamidino-2-phenylindole; DLL3, delta like protein 3; ERK, extracellular signal- regulated kinase.

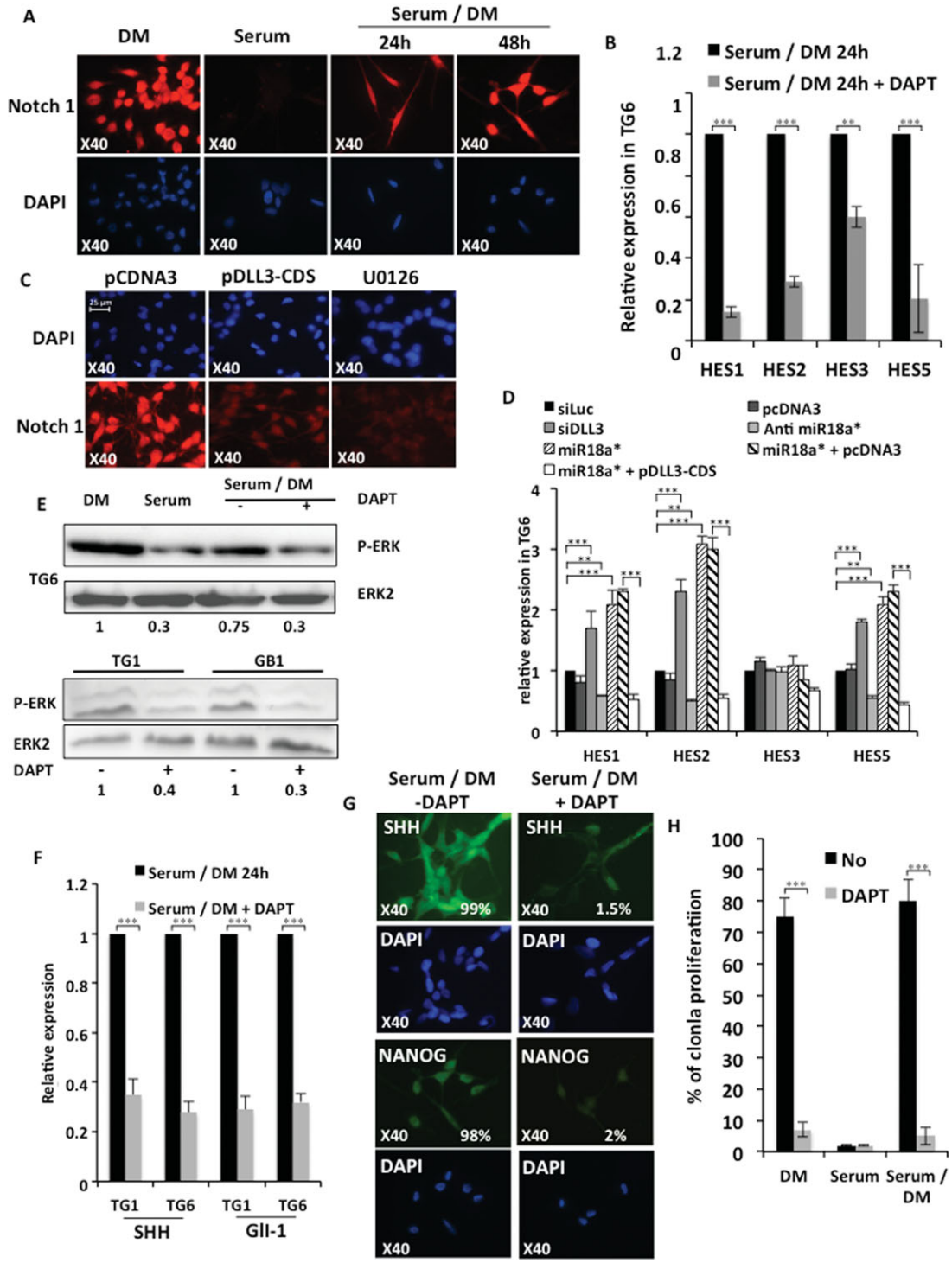

Figure 5. miR-18a*/delta like protein 3 (DLL3)-mediated NOTCH activation is required for ERK activation, sonic hedgehog (SHH)-Gli-NANOG network expression, and glioma initiating cell (GiC) clonal proliferation. **(A):** Immunostaining showing cleaved NOTCH1 expression in TG6 cells either cultured in DM, serum (serum), or serum for 4 days prior to defined medium for 24 or 48 hours. The nuclei were stained with DAPI. **(B):** Quantitative polymerase chain reaction (qPCR) shows relative HES mRNA expression in TG6 cultured for 4 days in serum prior to defined medium for 24 hours in the presence or absence of DAPT. Results are the average of three independent experiments. **(C):** Immunostaining showing the effects of DLL3 overexpression and ERK inhibition on cleaved NOTCH-1 expression. As indicated, TG6 cells, cultured in DM, were transfected with either pCDNA3 as control or pDLL3-CDS or treated with U0126 to inhibit ERK activity. **(D):** qPCR shows the level of HES mRNA in TG6 cells switched to defined medium for 24 hours and transfected either with siLuc, siDLL3, pcDNA3, synthetic miR-18a*, anti miR-18a*, and synthetic miR-18a*+ pDLL3-CDS. **(E):** Immunoblot analyses show phospho-ERK levels in TG6 cells (upper panels) cultured in DM, in serum, or in serum 4 days prior to being incubated in defined medium for 96 hours in the presence or absence of DAPT. Results for TG1 and GB1 cells switched to DM in the presence or absence of DAPT are shown in lower panels. **(F):** qPCR shows the impact of the inhibition of NOTCH-1 cleavage on SHH and GLI-1 mRNA levels, in TG6 or TG1 following the switch to defined medium for 24 hours. Results are the average of three independent experiments. **(G):** Similar conditions were used to show SHH and NANOG protein levels by immunostaining. Nuclei were stained with DAPI and confirm the presence of cells. **(H):** TG6 cells were cultured as single cells in DM in the presence or absence of DAPT, to assess their clonal proliferation efficiency. Hundred wells were counted for each condition, and the results are the average of four independent experiments. (***, p value $<.001$;**, p value $<.01$). Abbreviations: DM, defined medium; DAPI, 4′,6′-diamidino-2-phenylindole; DAPT, LY-374973, N-[N-(3,5-Difluorophenacetyl)-L-alanyl]-S-phenylglycine t-butyl ester; ERK, extracellular signal- regulated kinase.

Information Fig. S6B). Expectedly, and according to its repressor effect on DLL3 expression, miR-18a* invalidation significantly inhibited the level of HES1, 2, and 5 while its overexpression strengthened their expression (Fig. 5D; Supporting Information Fig. S6B). In addition, restoring DLL3 expression (pDLL3-CDS construct) abolished miR-18a*-mediated induction of HES1, 2, and 5 (Fig. 5D; Supporting Information Fig. S6B). These results demonstrate that NOTCH-1 activation in GiCs relies on miR-18a*-mediated downregulation of the DLL3 protein, and this mechanism is strongly dependent on ERK activation.

We demonstrated (Fig. 4G, 4H; Supporting Information Fig. 4F, 4G) that DLL3 and miR-18a* modulation impacts the activation of ERK. Since NOTCH-1 activation was found to be strongly dependent on DLL3 and miR-18a*, it is possible that the NOTCH pathway may contribute to ERK activation. Indeed, inhibition of NOTCH activation, using DAPT, upon switching cells to defined medium, repressed ERK phosphorylation (Fig. 5E) and consequently affected both miR-18a* and DLL3 expression (Supporting Information Fig. S6C, S6D). These results demonstrate that activated NOTCH constitutes a major miR-18a* effector for maintaining activated ERK. Accordingly, and since the ERK pathway is essential to turn on the SHH pathway (Fig. 2A–2C), inhibition of NOTCH activation, prevented SHH, GLI, NANOG expression at the mRNA and protein levels (Fig. 5F, 5G; Supporting Information Fig. S6E). siRNA-mediated knockdown of NOTCH-1 showed similar results, confirming the impact of NOCTH-1 activation on ERK phosphorylation as well as SHH, GLI and NANOG expression (Supporting Information Fig. S7). Consequently, invalidation of NOTCH signaling, led ineluctably to the loss of clonal proliferation (Fig. 5H; Supporting Information Fig. S6F). Taken together, our results demonstrate that miR-18a*, by downregulating the DLL3 protein, promotes NOTCH-1 activation, which in turn contributes to SHH-GLI-NANOG regulation, at least in part, through ERK activation (as schematized in Fig. 6A).

Status of MiR-18a*, DLL3, and SHH Expression in GBM Samples

We have demonstrated in culture that high miR-18a* levels positively correlate with increased clonal proliferation/tumorigenicity of GiCs and with the downregulation of DLL3 expression. To assess the miR-18a* status in GBM we performed in situ hybridization on surgical resections from human tumors. Five different cases are displayed in Figure 6B. Interestingly, miR-18a* staining revealed distinct territories containing more or less densely packed positively stained cells within the tumor. From our results, we would expect higher miR-18a* levels in cells which express lower levels of DLL3 protein. To test this hypothesis, we isolated tumor cells harboring low DLL3 levels and highly positive DLL3 cells from the same surgical resections and subjected them to RNA extraction and qPCR analysis. Consistent with our in vitro results using GICs, the data revealed twofold higher miR-18a* expression in cells displaying low DLL3 levels, as compared to highly DLL3-positive cells (Fig. 6C), suggesting that miR-18a*-mediated DLL3 regulation may occur within the tumor. Accordingly, higher levels of SHH, GLI-1, HES1 mRNAs were observed in cells with low DLL3 expression (Fig. 6C). Based on these results, it is likely that DLL3 downregulation within the tumor might lead, as observed in culture, to positive SHH protein regulation. We therefore analyzed SHH and DLL3 protein coexpression by immunofluorescence on sections of paraffin-embedded GBM from 10 different patients. Consistent with the low number of self-renewing cells within a tumor mass, the results revealed that SHH positive cells are much less frequent than SHH negative cells (Fig. 7A). Remarkably, all SHH positive cells were either negative for DLL3 or displayed very weak staining of the protein. Strikingly, highly positive DLL3 cells were all negative for SHH staining (Fig. 7A, 7B; Supporting Information Fig. S7A) confirming in vivo, the inverse correlation between DLL3 and SHH expression. Identical exclusion between DLL3 expression and the well-known neural stem cell marker SOX2 (Fig. 7A and 7B) or SOX1 also associated with neural stem cells [24–26] (Supporting Information Fig. S7B, S7C) further confirmed the inverse correlation between DLL3 expression and stemness.

Discussion

In this study, we have demonstrated the contribution of miR-18a* to the promotion of GiC self-renewal and tumorigenicity through NOTCH-1 activation. In addition, we found that miR-18a*-mediated NOTCH-1 activation, in that context, was absolutely required for expression and activation of the SHH-GLI-NANOG regulatory network, previously described as essential for GiC self-renewal and expression of an embryonic stem cells (ES)-like signature [14, 15]. Furthermore, we have demonstrated that not only miR-18a* expression but also NOTCH-1 activation and clonal proliferation, rely on ERK phosphorylation (schematized in Fig. 6A).

Although MAPK/ERK signaling has previously been implicated in promoting the spontaneous differentiation of mouse embryonic stem cells [27] or maintenance of the differentiated state of somatic cells [28], its requirement for adult neural stem cell self-renewal [29, 30] as well as its regulation of the Hedgehog pathway [21] has recently been reported. Consistently, our results demonstrate that, by regulating SHH and GLI expression levels, MAPK/ERK constitutes a major player for controlling the SHH-GLI-NANOG regulatory network and thereby GiC self-renewal. In self-renewing conditions, we found that miR-18a* expression was dependent on ERK activation. This result is in good agreement with recent reports, demonstrating that production of growth-promoting miRNA arises through pERK1/2-mediated phosphorylation of TRBP protein, a member of the miRNA generating complex [19]. miR-18a* belongs to the "miR-17 approximately 92" cluster. While members of this cluster are known to have growth-promoting effects [30, 31], miR-18a* has also been described as a putative tumor suppressor through the repression of K-Ras [32]. However, its regulation and contribution to the control of cancer stem cell self-renewal and tumorigenicity has not yet been reported. In our primary GiCs cultures, miR-18a* constitutes an important effector of ERK since its inhibition strongly repress expression of SHH, GLI, and NANOG proteins, thus compromising integrity of the SHH-GLI-NANOG regulatory network. Conversely, ectopic miR18a* overexpression leads to the opposite effect and clearly strengthens SHH, GLI, NANOG expression and enhances GiC tumorigenicity in intracranial xenograft experiments. Thus, modulation of miR-18a* expression and ERK activity induce similar effects on the SHH pathway and NANOG expression. The relationship between these two elements is further reinforced by a positive feedback loop in which ERK1/2 phosphorylation is augmented by miR-18a*, and miR-18a* expression is dependent on ERK activation. However, even if miR-18a* plays a prominent role in the control of the SHH-GLI-NANOG regulatory network, the rescue of its expression is not sufficient

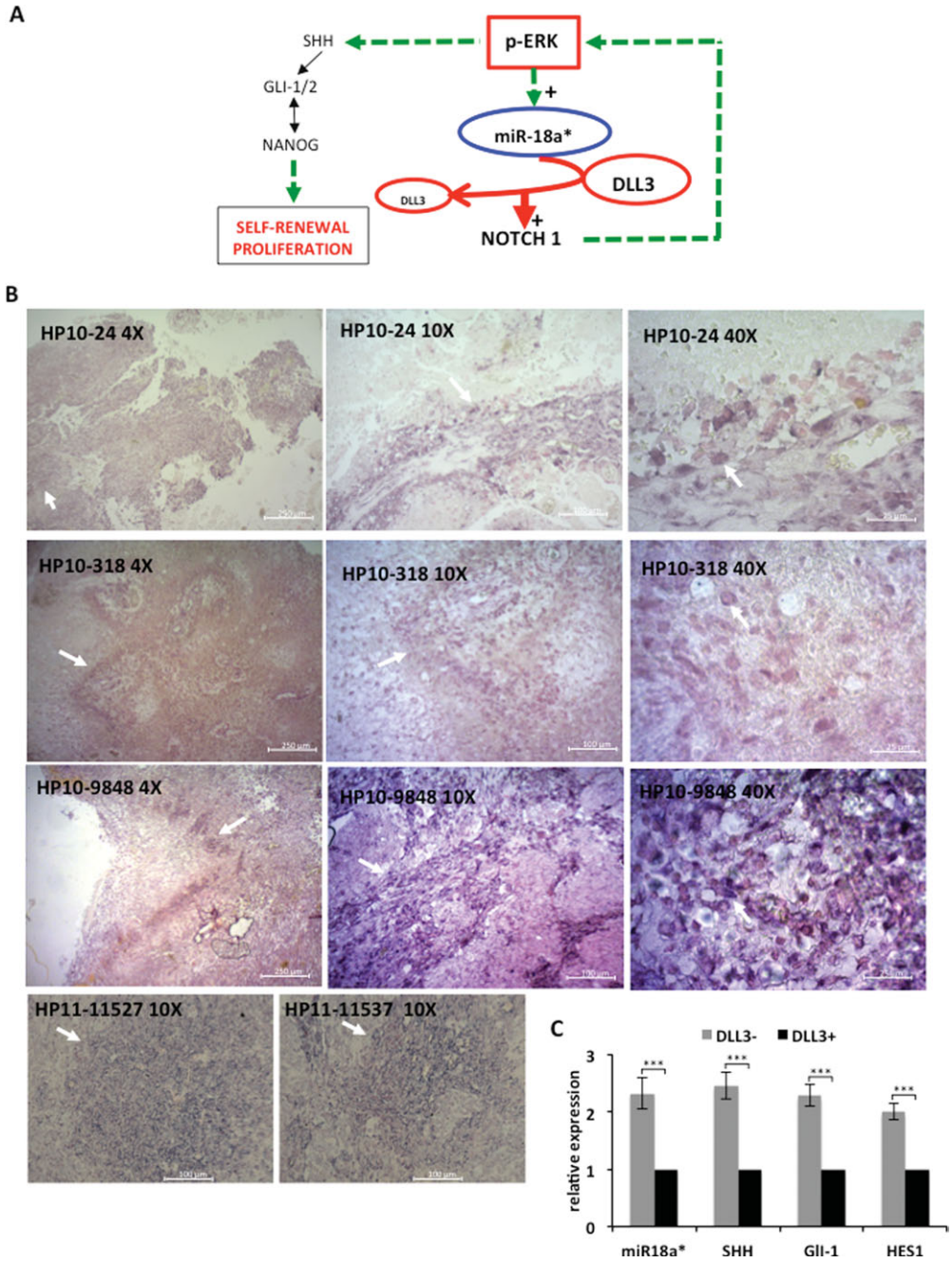

Figure 6. miR-18a* expression in glioblastoma (GBM) samples. **(A):** Cartoon showing the miR-18a*-dependent molecular pathway involved in the control of clonal proliferation. Arrows indicate direct regulations. Dash arrows indicate the effects of NOTCH-1 and MAPK activation on MAPK and SHH signaling. **(B):** In situ hybridization showing miR-18a* expression in GBM paraffin sections (purple staining, white arrow). Scale bars are shown in the pictures. **(C):** Four different GBM samples (HP10-24, HP10-9848, HP11-11527, and HP11-537) were dissociated, and cells expressing low DLL3 levels were separated from cells expressing high DLL3 levels. Total RNAs were prepared for both cell populations and miR-18a*/SHH/GLI-1/HES1 expression was measured by quantitative polymerase chain reaction. The data are the meaning of the results obtained for each sample (***, p value $<.001$). Abbreviations: ERK, extracellular signal-regulated kinase; SHH, sonic hedgehog.

to bypass ERK inhibition. This places ERK at a central place for the control of GiC self-renewal. In that context, we have demonstrated that miR-18a* directly downregulates expression of DLL3 protein. Importantly, we showed that DLL3 silencing has the same effect on ERK activity and the SHH pathway, as miR-18a* overexpression. DLL3 is a divergent member of the DSL family of NOTCH ligands that does not activate signaling but instead inhibits NOTCH signaling when expressed in the same cell as the NOTCH receptor [21, 22]. In this study, we confirmed the inhibitory potential of DLL3 on NOTCH-1 activity in GiCs. Consistent with other reports, describing that NOTCH-1 pathway blockade depletes CD133-positive GBM cells [12], our results clearly demonstrate its requirement for self-renewal of primary GiC cultures. We further demonstrate here that inhibition of NOTCH-1 activation clearly compromises ERK

A

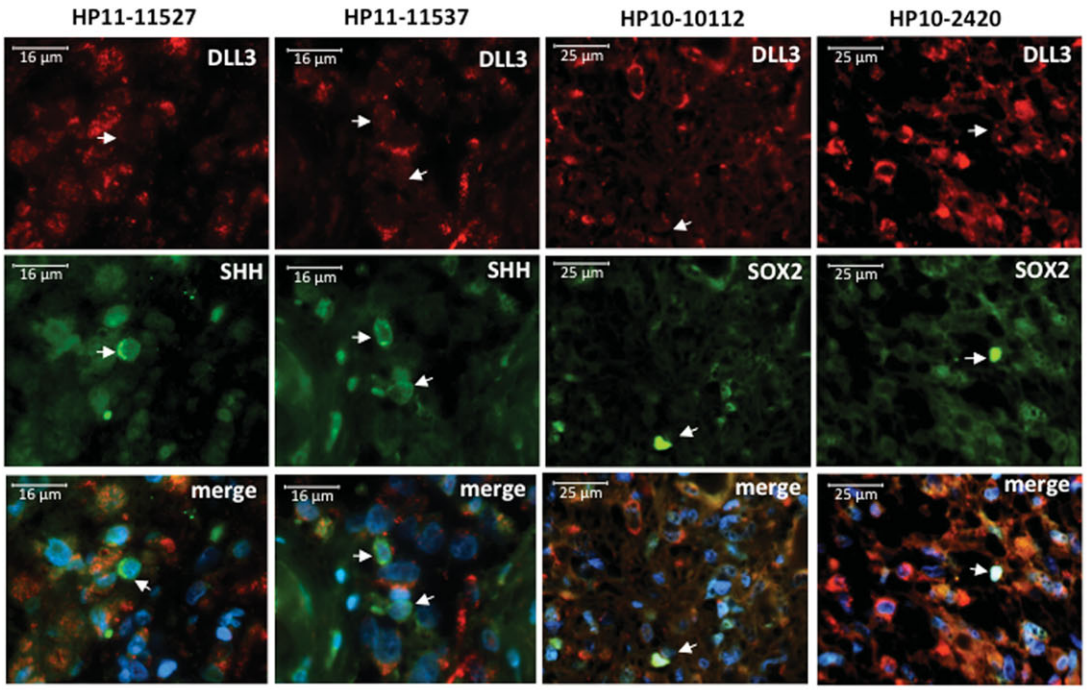

B

CASES	cells nbr	SHH+/ DLL3- or weakly +	SHH+/ DLL3+	SHH-/ DLL3+	SHH-/ DLL3-	cells nbr	SOX2+/ DLL3- or weakly +	SOX2+/ DLL3+	SOX2-/ DLL3+	SOX2-/ DLL3-
HP11-11527	350	18 (5.1%)	0	170 (48.6%)	162 (46.3%)	553	10 (1.8%)	0	276 (49.9%)	277 (50.1%)
HP11-11537	298	20 (6.7%)	0	147 (49.3%)	131 (44%)	345	4 (1.2%)	0	198 (57.4%)	147 (42.6%)
HP10-2132	225	10 (4.4%)	0	112 (49.8%)	103 (45.8%)	657	15 (2.3%)	0	298 (45.4%)	359 (54.6%)
HP10-24	234	15 (6.4%)	0	114 (48.7%)	105 (44.9%)	520	13 (2.5%)	0	239 (46%)	281 (54%)
HP10-318	201	7 (3.5%)	0	90 (44.8%)	104 (51.7%)	435	14 (3.2%)	0	212 (48.7%)	223 (51.3%)
HP10-2024	225	12 (5.3%)	0	111 (49.3%)	102 (45.3%)	603	11 (1.8%)	0	289 (47.9%)	314 (52.1%)
HP11-9890	365	23 (6.3%)	0	181 (49.6%)	161 (44.1%)	465	17 (3.7%)	0	254 (54.6%)	211 (45.4%)
HP10-9248	226	16 (7.1%)	0	130 (57.5%)	80 (35.4%)	877	14 (1.6%)	0	176 (20.1%)	701 (79.9%)
HP10-10112	154	6 (3.9%)	0	87 (56.5%)	61 (39.6%)	344	16 (4.6%)	0	134 (39%)	210 (61%)
HP10-12916	281	5 (1.8%)	0	91 (32.4%)	185 (65.8%)	456	9 (2.2%)	0	102 (22.4%)	354 (77.6%)

Figure 7. Inverse correlation between DLL3 and SHH or SOX2 expression in glioblastoma (GBM) samples. **(A):** Immunofluorescence staining shows DLL3 (red) and SHH (green) or SOX2 (green) coexpression in paraffin sections of human GBM. Nuclei were stained with 4′,6′-diamidino-2-phenylindole (blue). White arrows show the SHH or SOX2 positive cells. Scale bars are shown in the pictures. **(B):** Quantification of the SHH+ DLL3− cells, SHH+ DLL3+ cells, SHH− DLL3+, and SHH− DLL3− cells or SOX2+ DLL3− cells, SOX2+ DLL3+ cells, SOX2− DLL3+, and SOX2− DLL3− cells in 10 different GBM cases. Percentage represents the partitioning of each cell population within the tumor. Five independent fields per case have been counted. Abbreviation: DLL3, delta like protein 3.

Table 1. % of CFSE positive cells in TG1, TG6, GB1, GB3 cultured in serum for 4 days or undergoing the switch from serum to DM for 48 hours

% of CFSE+ cells	TG1	TG6	GB1	GB3
Serum 4 days	96.04 ± 1.59	95.34 ± 1.54	94.78 ± 3.34	93.49 ± 0.93
Serum/DM 48h	95.30 ± 2.38	96.31 ± 2.90	94.85 ± 1.25	96.71 ± 2.44

Abbreviations: CFSE, carboxyfluorescein diacetate, succinimidyl ester; DM, defined medium.

activity and consequently the SHH-GLI-NANOG regulatory network. This is consistent with other reports, which describe a pro-survival role of NOTCH signaling through activation of the ERK pathway [33]. By decreasing DLL3 protein levels, miR-18a* strengthens NOTCH-1 signaling, which in turn activates ERK, thereby inducing SHH and GLI expression. Activated NOTCH-1 acts as miR-18a* effector for the positive feedback loop for fine-tuning of constitutive and basal activated ERK. Thus, miR-18a*-mediated DLL3 regulation constitutes an important signaling event for controlling the switch between the self-renewing and non-self-renewing state. We have extended our observations to human tumor samples. Indeed, miR-18a* expression was detected by in situ hybridization in GBM sections. Interestingly miR-18a* expression was approximately two times higher in tumor cells expressing low level of DLL3 as compared to highly positive DLL3 cells thus corroborating our in vitro data. We further demonstrated, in several GBM samples, that SHH expression is detected only in cells harboring negative or low level of DLL3 protein.

Conclusion

In conclusion, our study reveals a miR-18a*/DLL3-dependent interplay between ERK and NOTCH-1 pathways, responsible for GiC self-renewal and tumorigenicity. GBM is the most aggressive brain tumor against which conventional therapies only provide transient clinical response always followed by tumor recurrence. In this context of therapeutic challenge, miR-18a* and DLL3 may be putative targets for the design of innovative treatment interfering with cancer growth and recurrence.

Acknowledgments

This work was supported by grants from the Association pour la Recherche sur le Cancer (subvention 3161), Association Sauvons Laura, Agence Nationale pour la Recherche (ANR Jeunes Chercheurs, Jeunes Chercheuses, ≪ GLIOMIRSTEM project ≫), Fondation de France, ARC projet, INSERM, UNSA. We thank Arnaud Borderie, Sandrine Bestrée, and Coralie Hagnere for technical assistance and Pr. J.F. Michiels is gratefully acknowledged for helpful comments on the study. We thank Dr. P. Lenormand for providing us with sh-ERK1 and sh-ERK2.

Disclosure of Potential Conflicts of Interest

The authors indicate no potential conflicts of interest.

References

1 Visvader JE, Lindeman GJ. Cancer stem cells in solid tumours: Accumulating evidence and unresolved questions. Nat Rev Cancer 2008;8:755–768.
2 Murat A, Migliavacca E, Gorlia T et al. Stem cell-related "self-renewal" signature and high epidermal growth factor receptor expression associated with resistance to concomitant chemoradiotherapy in glioblastoma. J Clin Oncol 2008;26:3015–3024.
3 Stupp R, Hegi ME. Targeting brain-tumor stem cells. Nat Biotechnol 2007;25:193–194.
4 Hope KJ, Jin L, Dick JE. Acute myeloid leukemia originates from a hierarchy of leukemic stem cell classes that differ in self-renewal capacity. Nat Immunol 2004;5:738–743.
5 Ponti D, Costa A, Zaffaroni N et al. Isolation and in vitro propagation of tumorigenic breast cancer cells with stem/progenitor cell properties. Cancer Res 2005;65:5506–5511.
6 Schatton T, Murphy GF, Frank NY et al. Identification of cells initiating human melanomas. Nature 2008;451:345–349.
7 Galli R, Binda E, Orfanelli U et al. Isolation and characterization of tumorigenic, stem-like neural precursors from human glioblastoma. Cancer Res 2004;64:7011–7021.
8 Chen R, Nishimura MC, Bumbaca SM et al. A hierarchy of self-renewing tumor-initiating cell types in glioblastoma. Cancer Cell 2010;17:362–375.
9 Prestegarden L, Svendsen A, Wang J et al. Glioma cell populations grouped by different cell type markers drive brain tumor growth. Cancer Res 2010;70:4274–4279.
10 Ogden AT, Waziri AE, Lochhead RA et al. Identification of A2B5+CD133− tumor-initiating cells in adult human gliomas. Neurosurgery 2008;62:505–514, discussion 514–505.
11 Wang J, Sakariassen PO, Tsinkalovsky O et al. CD133 negative glioma cells form tumors in nude rats and give rise to CD133 positive cells. Int J Cancer 2008;122:761–768.
12 Fan X, Khaki L, Zhu TS et al. NOTCH pathway blockade depletes CD133-positive glioblastoma cells and inhibits growth of tumor neurospheres and xenografts. Stem Cells 2010;28:5–16.
13 Karsy M, Albert L, Tobias ME et al. All-trans retinoic acid modulates cancer stem cells of glioblastoma multiforme in an MAPK-dependent manner. Anticancer Res 2010;30:4915–4920.
14 Clement V, Sanchez P, de Tribolet N et al. HEDGEHOG-GLI-1 signaling regulates human glioma growth, cancer stem cell self-renewal, and tumorigenicity. Curr Biol 2007;17:165–172.
15 Zbinden M, Duquet A, Lorente-Trigos A et al. NANOG regulates glioma stem cells and is essential in vivo acting in a cross-functional network with GLI-1 and p53. EMBO J 2010;29:2659–74.
16 Fareh M, Turchi L, Virolle V et al. The miR 302–367 cluster drastically affects self-renewal and infiltration properties of glioma-initiating cells through CXCR4 repression and consequent disruption of the SHH-GLI-NANOG network. Cell Death Differ 2012;19:232–244.
17 Patru C, Romao L, Varlet P et al. CD133, CD15/SSEA-1, CD34 or side populations do not resume tumor-initiating properties of long-term cultured cancer Stem Cells from human malignant glio-neuronal tumors. Bmc Cancer 2010;10:66.
18 Verhaak RG, Hoadley KA, Purdom E et al. Integrated genomic analysis identifies clinically relevant subtypes of glioblastoma characterized by abnormalities in PDGFRA, IDH1, EGFR, And NF1. Cancer Cell 2010;17:98–110.
19 Paroo Z, Ye X, Chen S et al. Phosphorylation of the human microRNA-generating complex mediates MAPK/Erk signaling. Cell 2009;139:112–122.
20 Lefloch R, Pouyssegur J, Lenormand P. Single and combined silencing of ERK1 and ERK2 reveals their positive contribution to growth signaling depending on their expression levels. Mol Cell Biol 2008;28:511–527.
21 Seto M, Ohta M, Asaoka Y et al. Regulation of the hedgehog signaling by the mitogen-activated protein kinase cascade in gastric cancer. Mol Carcinog 2009;48:703–712.
22 Chapman G, Sparrow DB, Kremmer E et al. Notch inhibition by the ligand DELTA-LIKE 3 defines the mechanism of abnormal vertebral segmentation in spondylocostal dysostosis. Hum Mol Genet 2011;20:905–916.
23 Hoyne GF, Chapman G, Sontani Y et al. A cell autonomous role for the Notch ligand Delta-like 3 in alphabeta T-cell development. Immunol Cell Biol 2011;89:696–705.
24 Alcock J, Sottile V. Dynamic distribution and stem cell characteristics of Sox1-expressing cells in the cerebellar cortex. Cell Res 2009;19:1324–1333.
25 Elkouris M, Balaskas N, Poulou M et al. Sox1 maintains the undifferentiated state of cortical neural progenitor cells via the suppression of Prox1-mediated cell cycle exit and neurogenesis. Stem Cells 2011;29:89–98.
26 Salcido CD, Larochelle A, Taylor BJ et al. Molecular characterisation of side population cells with cancer stem cell-like characteristics in small-cell lung cancer. Br J Cancer 2010;102:1636–1644.
27 Ying QL, Wray J, Nichols J et al. The ground state of embryonic stem cell self-renewal. Nature 2008;453:519–523.
28 Lluis F, Cosma MP. Somatic cell reprogramming control: Signaling pathway modulation versus transcription factor activities. Cell Cycle 2009;8:1138–1144.
29 Lee JA, Jang DJ, Kaang BK. Two major gate-keepers in the self-renewal of neural stem cells: Erk1/2 and PLCgamma1 in FGFR signaling. Mol Brain 2009;2:15.

30 Ma DK, Ponnusamy K, Song MR et al. Molecular genetic analysis of FGFR1 signalling reveals distinct roles of MAPK and PLCgamma1 activation for self-renewal of adult neural stem cells. Mol Brain 2009; 2:16.
31 Takakura S, Mitsutake N, Nakashima M et al. Oncogenic role of miR-17–92 cluster in anaplastic thyroid cancer cells. Cancer Sci 2008; 99:1147–1154.
32 Tsang WP, Kwok TT. The miR-18a* microRNA functions as a potential tumor suppressor by targeting on K-Ras. Carcinogenesis 2009;30: 953–959.
33 Liu ZJ, Xiao M, Balint K et al. Notch1 signaling promotes primary melanoma progression by activating mitogen-activated protein kinase/ phosphatidylinositol 3-kinase-Akt pathways and up-regulating N-cadherin expression. Cancer Research 2006;66:4182–4190.


See www.StemCells.com for supporting information available online.